

Evolution of mean wind and turbulence fields in a quasi-baroclinic convective boundary layer with strong wind shears

Robert J. Conzemius^{a,1}, Evgeni Fedorovich^a

^a*School of Meteorology, University of Oklahoma, 100 E. Boyd, Norman, OK, USA*

ABSTRACT: The growth of the atmospheric convective boundary layer (CBL) is forced mostly by buoyancy production at the surface. However, wind shear has a significant impact on the turbulence structure within the CBL and can contribute significantly to CBL growth when mean winds or wind shear in the lower atmosphere are strong and buoyancy flux from the surface and stratification in the free atmosphere above are both weak. Regimes of CBL growth in calm (shear-free), windy, and strong wind shear cases were studied using large eddy simulation (LES). The study evaluated the effects of shear on the CBL growth rate, the evolution of mean wind profiles within the CBL, and semi-organized and turbulent flow structures.

KEYWORDS: convective boundary layers, wind shear, turbulence.

1 INTRODUCTION

The boundary layer is the layer of the atmosphere, closest to the ground, which “feels” the effects of mass, momentum, and heat exchanges with the surface on time scales of about one hour or less. As such, it is a layer in which a significant amount of active mixing occurs. The wind speed near the surface is heavily influenced by mixing processes within the boundary layer. The prediction of boundary layer winds is important for the wind energy industry. The present study focuses on the convective boundary layer (CBL), in which the turbulent mixing is forced by heating of the underlying surface. Due to this mixing, the effects of surface friction can be felt over a rather substantial depth of the CBL. At the same time, the turbulent convection is also rather effective at transporting momentum from aloft to the surface. This paper discusses features of the mean flow and turbulence structure of the CBL with different extents of wind shear contribution to momentum transport across the layer. The observation and prediction of winds in the CBL have been the subject of numerous publications (e.g. [1],[2],[3],[4],[5],[6], and [7]). The CBL winds were found to be dependent on the geostrophic forcing (defined below), changes in the geostrophic forcing with height, the depth of the CBL, and the rate at which the CBL grows.

1.1 *Geostrophic forcing in baroclinic and barotropic boundary layers*

In much of the atmosphere, the wind is in geostrophic balance, which is a balance between the horizontal pressure gradient force and the Coriolis force. The wind resulting from this balance is referred to as the geostrophic wind. The geostrophic wind speed is proportional to the horizontal component of the pressure gradient force, and its direction is perpendicular to the pressure gradient with lower pressure to the left of the wind vector in the Northern Hemisphere and right of the wind vector in the Southern Hemisphere. If there is no change in the geostrophic wind direction or speed with height, the atmosphere is referred to as barotropic. The speed and direction of the geostrophic wind can change as a function of height in the atmosphere due to baroclinicity. For instance, if a horizontal temperature gradient exists that is not aligned with the pressure gradient (this situation is commonly observed near atmospheric fronts), the geostrophic wind will change

with height, and shear in the geostrophic wind will be found. A boundary layer under such conditions is referred to as a baroclinic boundary layer. The shear in the geostrophic wind, as well as the overall speed of the wind can affect the rate at which the CBL grows during the day, and this, in turn, can affect the wind field within the CBL.

1.2 *Daytime evolution of the CBL*

The CBL typically grows slowly in the early morning as surface heating commences, and the growth occurs through a shallow inversion that has developed at the surface during the preceding night. As the surface heating increases in the late morning and the inversion is eroded, the CBL grows much more rapidly through the so-called residual boundary layer (from the previous day's CBL), which is rather weakly stratified. It is at this stage that surface winds increase most dramatically, as higher momentum air is mixed down from aloft. The CBL then usually reaches a strong inversion farther aloft, which considerably slows its growth in the midday to early afternoon, but the strong surface winds continue for most of the day. During the late afternoon, surface heating weakens, and eventually, the heat flux convergence at the surface becomes zero and then negative, forcing cooling near the surface and the decoupling of winds in the early evening. At this point, surface winds decrease, while winds aloft can remain rather strong and, in most cases, increase again, since the effects of surface friction no longer slow them.

1.3 *Effects of wind speed and shear on the development and structure of the CBL*

In most cases, the development of the CBL is primarily forced by heating of the underlying surface, which follows the daily cycle described above. In such situations, the CBL growth is driven by the surface heating and the stratification in the atmosphere above the CBL (see [11]). In some cases, however, strong winds can generate additional turbulent mixing, which can enhance the CBL growth. If this occurs, stronger winds will be brought to the surface by the mixing effects of the deeper CBL. Because the convective turbulence mixes momentum rather effectively, wind shear within the CBL is typically concentrated near the surface and at the top of the CBL. The proportion of the shear that exists at the surface versus the CBL top is governed by the geostrophic shear (described above) and the time over which the CBL growth occurs. These wind shears have a significant effect on the flow structure within the CBL. Several studies ([8],[9],[10]) have already documented such structures in cases with both light winds and strong winds, including studies by Moeng & Sullivan [8], Khanna & Brasseur [9], and Schmidt & Schumann [10]. Typically, the convective elements within the CBL form into hexagonally shaped cells when the winds are light and horizontal rolls when winds are strong. These features have been well described in the aforementioned studies. The goal of this paper is to further investigate the effects of wind shear at the surface and the top of the CBL on the CBL growth and the resulting feedbacks in the evolution of the mean wind and turbulence structures within the CBL.

2 EXPERIMENTAL SETUP

2.1 *Cases investigated*

The cases investigated in this study spanned a wide range of surface heat flux, free atmosphere stratification, and wind shear conditions. The wind speed and shear were divided into three primary regimes: (i) a case with no geostrophic wind (NS), in which mean wind was zero throughout the depth of the CBL, (ii) a barotropic case, in which the initial wind was in geostrophic balance at 20m/s (GC), and (iii) a baroclinic case, in which the geostrophic wind varied from zero at

the surface to 20m/s at the top of the model domain (GS). In all these cases, the geostrophic forcing was kept constant with time. The surface heat flux, expressed in terms of kinematic temperature flux, was set to 0.03 Km/s, 0.1 Km/s, or 0.3 Km/s. Finally, the free-atmosphere stratification was given values of 0.001 K/m, 0.003 K/m, or 0.010 K/m. The degrees of freedom in these parameters result in an array of 24 individual cases that were simulated within this experiment. Table 1 shows the cases that were simulated.

Table 1. Cases simulated in this study

Stratification (K/m)	Surface heat flux (K·m/s)		
	0.03	0.10	0.30
0.010		×	×
0.003	×	×	×
0.001	×	×	×

× indicate setups for which all three shear cases (NS,GS,GC) were simulated

2.2 Large Eddy Simulation methodology

All cases listed in Table 1 were investigated numerically by means of large eddy simulation (LES). The LES code used in this study has its origins in studies performed by Deardorff [12], Wyngaard & Brost [13], and Nieuwstadt & Brost [14] and is described in detail in these references. The specifications of the grid, domain, boundary conditions, and other LES parameters for the present study are listed in Table 2.

Table 2. LES parameters

Parameter	Specification
Domain size	5.12x5.12x1.6 km
Grid	256x256x80 (20 meter cells)
Bottom boundary condition for wind and temperature	Local Monin-Obukhov similarity
Top boundary condition	Neumann (zero gradient)
Sponge layer	Top 20% of domain
Lateral boundary condition	Periodic
Subgrid turbulence parameterization	Deardorff (1.5-order, subgrid TKE closure)
Initial perturbation	2 K (temperature)
Initial CBL depth	0

The geostrophic wind and wind shear in the LES were implemented in the form of a geostrophic term in the equations of motion that was allowed to vary with height. The model atmosphere is not truly baroclinic, since a mean horizontal temperature gradient cannot be represented within the confines of periodic boundary conditions. Statistics were calculated over horizontal planes in the model domain with no time averaging involved. These statistics included first and second order moments of all scalar and momentum fields, as well as third order moments of temperature and vertical velocity.

3 RESULTS

3.1 Mean Wind Profiles

The mean wind profiles within the CBL change under the influence of the surface friction and downward transfer of momentum from the CBL top. Figure 1 shows the mean x -component of wind (u) for the GC case with free-atmosphere stratification of 0.010 K/m and surface kinematic temperature flux of $0.3 \text{ K}\cdot\text{m/s}$. The CBL evolution starts out with shear concentrated mostly in the surface layer, with little shear across the CBL top. However, as the CBL grows, the effects of surface friction are seen over a deeper layer, and the CBL mean wind decreases over the course of several hours. As this occurs, wind shear across the CBL top increases while the surface shear slowly decreases. The mean CBL wind stays equal to or less than the geostrophic wind speed for all times in Figure 1a.

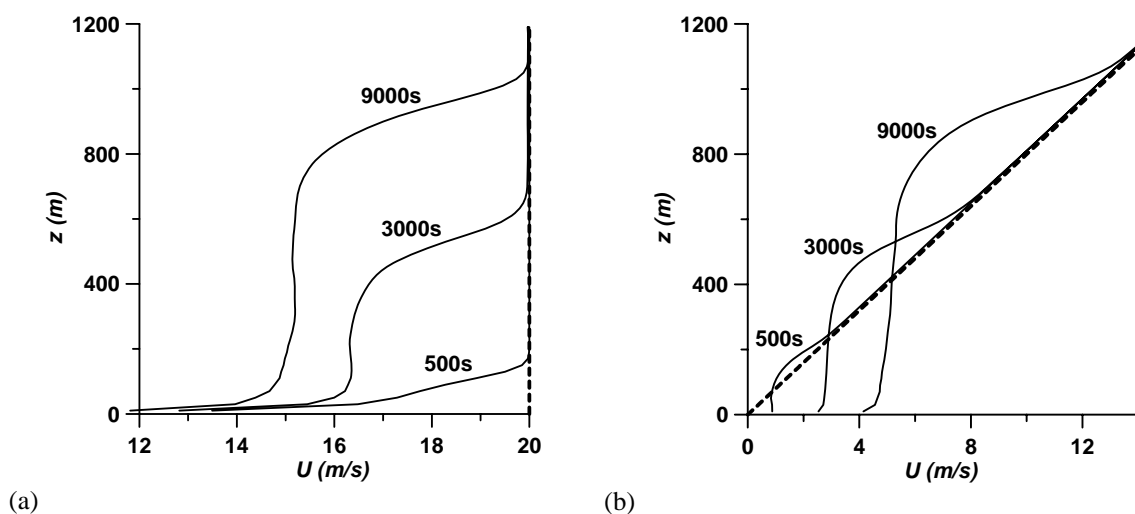


Figure 1. Mean wind profiles for (a) the GC case and (b) the GS case for $d\theta/dz=0.01 \text{ K/m}$ and $Q_s=0.3 \text{ K}\cdot\text{m/s}$ at selected times during the simulation. Dashed lines represent the original profiles at $t=0$.

Figure 1b shows the evolution of u for the GS case. Given the shear in the geostrophic wind, the bulk of the shear is immediately found at the CBL top. As the CBL grows, it encounters increasingly strong winds at its top, and this momentum is transferred downward into the CBL. Initially, the surface shear is zero, but as downward transfer of momentum proceeds, the wind speed near the surface exceeds its geostrophic value, and surface shear builds. This increase in surface wind speed is offset by the decrease in the wind speed at higher levels, particularly as the CBL grows into the levels with stronger winds. In these levels, the wind speed drops below its geostrophic value.

3.2 CBL growth

The evolution of the wind profiles depends also on the rate of growth of the CBL. Strong shear can have a significant effect on the growth rate of the CBL when buoyancy flux at the lower surface is weak and if the stratification of the atmosphere above the CBL is moderate or weak. Figure 2 shows the overall CBL depth as a function of time for nine of the simulated cases, with strongest buoyancy forcing in Figure 2a and weakest buoyancy forcing in Figure 2c. It is evident that the shear can have a significant effect on the CBL growth, but if buoyancy flux and the atmospheric stratification are both strong, the effects of shear, in a relative sense, become negli-

ble. Nevertheless, shear still exerts a strong influence over the turbulence structures within the CBL (see Section 3.6).

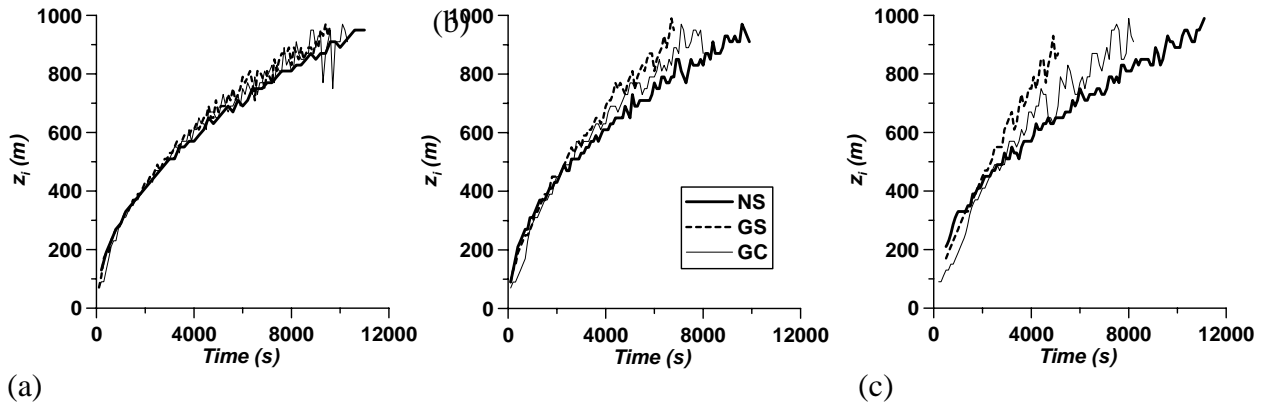


Figure 2. CBL depth, z_i , as a function of time for cases with (a) strong, (b) moderate, and (c) weak forcing by buoyancy.

3.3 Effects of CBL growth rate on mean wind profiles

The mean wind profiles for selected GC simulations are shown in Figure 3a and, for selected GS cases, in Figure 3b. In all these cases, the profiles were taken at a time in the simulation when the CBL depth was approximately 680 meters. In Figure 3a, one can see that the effects of surface friction are stronger when slower CBL growth occurs. The runs with weaker surface buoyancy flux and stronger atmospheric stratification require more time for the CBL to grow, and hence, the surface shear effects accumulate. In the GS case (Fig. 3b), however, the main effect of the CBL growth rate is seen through the degree of mixing of momentum within the CBL. For cases in which the CBL grows slowly, the momentum is well mixed in the CBL, and surface shear and shear at the CBL top are nearly equivalent. However, rapid CBL growth results in momentum fields that are not well mixed within the CBL, because in this case the CBL grows more quickly than these fields get mixed by convective motions [5].

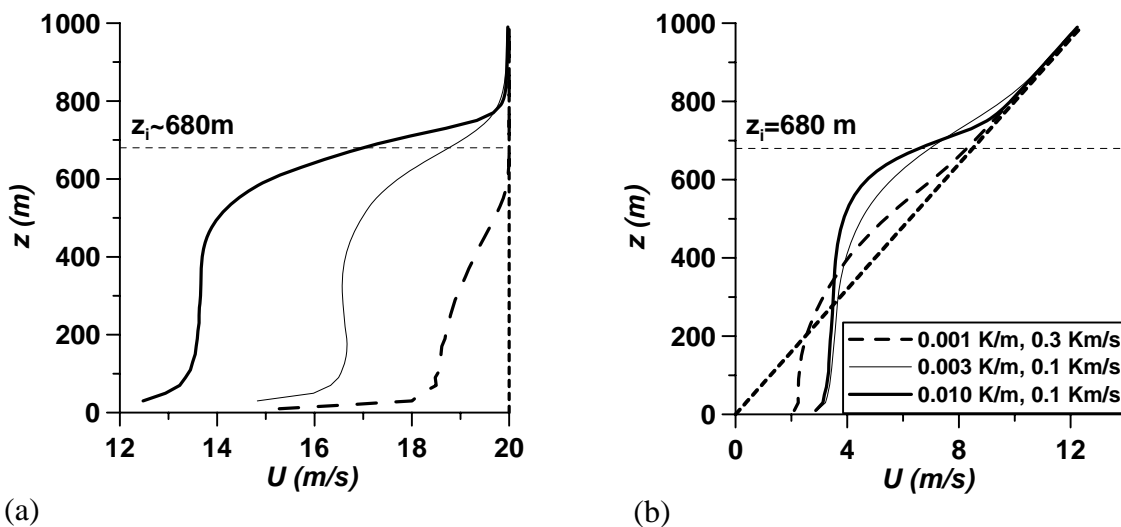


Figure 3. Evolution of wind profiles affected by CBL growth rate for (a) GC cases and (b) GS cases when the CBL depth was 680m in the simulations.

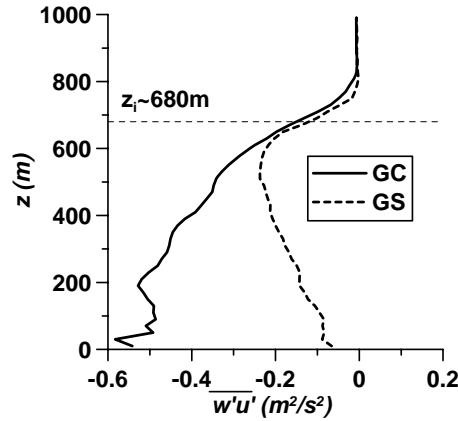


Figure 4. Turbulent stress profiles of u for the GC and GS cases 4700s into the simulation. $d\theta/dz=0.010$ K/m and $Q_s=0.3$ Km/s

3.4 Turbulence statistics

Figure 4 shows profiles of the x component of momentum flux. For the GC case, the profiles are indicative of generally slowing winds in the CBL, with the magnitude of momentum flux decreasing with height. Within the bottom 200 meters of the simulation, the vertical changes of flux are small, which indicates that friction is not doing much to change u there. For the GS case, the flux convergence from the surface up to 600 m is positive, indicating an acceleration of the x component of wind in most of the CBL. In fact, this is exactly what happens in this case after the winds are first slowed at the top of the boundary layer, according to Figure 1b. As the CBL grows, it removes momentum from the upper portion of the CBL and places it in the lower portion. For the wind at any given level, the winds first decrease as they encounter the top of the growing CBL. After they have decreased a bit, they again begin to increase as the CBL grows into regions with much stronger winds and transports this momentum downward.

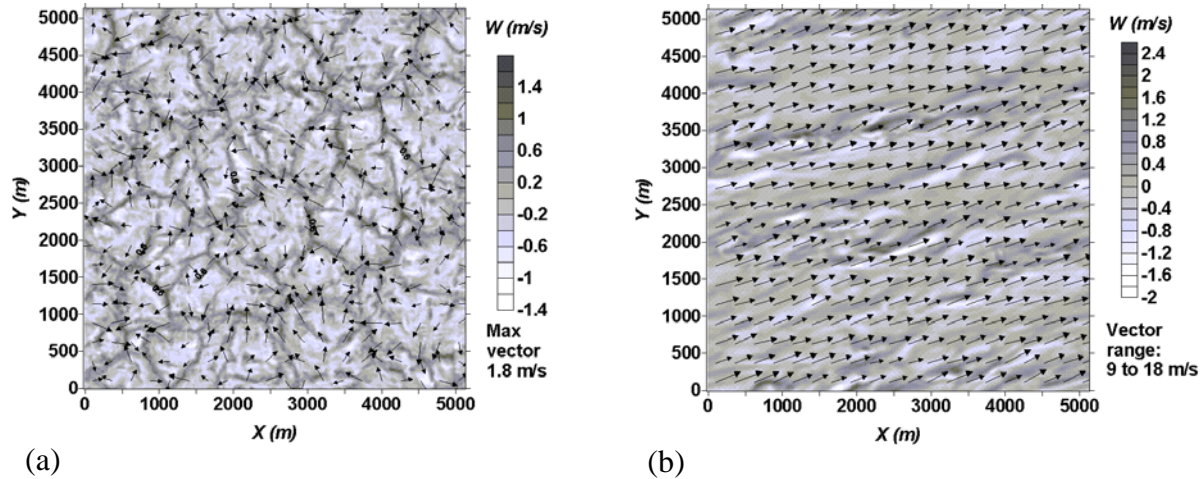
3.5 Turbulent structures within the CBL affected by shear

Figure 5 shows the structure of the simulated convection in the NS case near the surface. (u, v, w plot) As has been shown in several studies in the past ([8],[9],[10]), with low winds (NS case) the convection organizes into quasi-hexagonal cell structures, with flow converging on the intersections between these cells, particularly where the lines of the hexagon intersect. However, in presence of wind, as in the GC case, the convective motion is formed into horizontal rolls oriented along the mean flow. As the CBL continues to grow, particularly when the surface buoyancy flux is strong, the rolls begin to transition into cells as the buoyancy forcing becomes relatively more important.

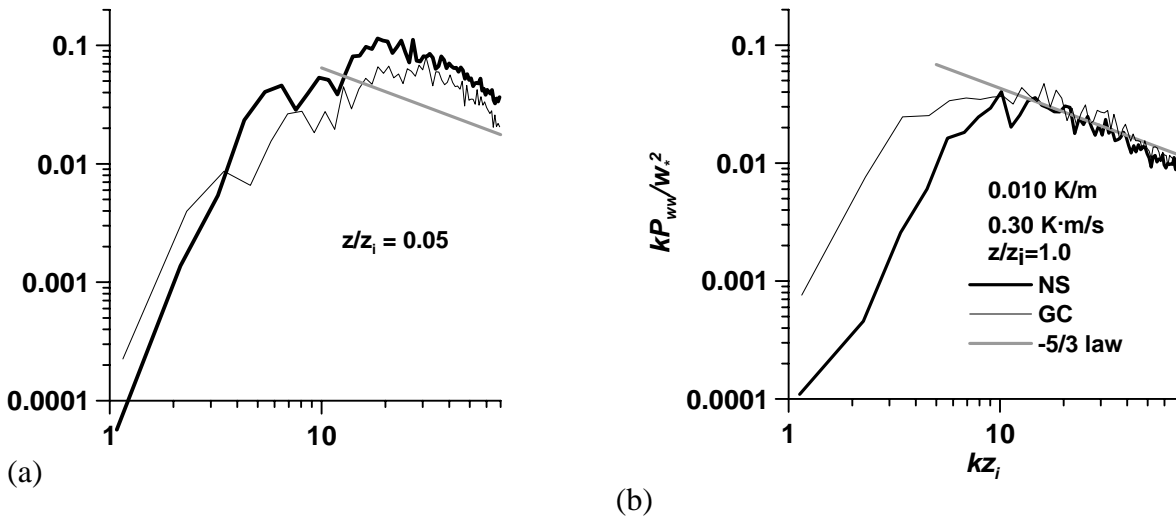
3.6 Turbulence spectra

Figure 6 shows the one-dimensional spectra of vertical velocity for the NS and GC cases with stratification of 0.010 K/m and a kinematic temperature flux of 0.3 Km/s. The profiles show that, despite the significantly different visual appearance of the structures of turbulence, the spectra are not greatly different. There are still some minor differences. Near the surface, the vertical ve-

locity variance is somewhat less for the GC cases than for the NS case, and this may be attributable to the smoothing and deforming effects of shear on convective structures as they develop near the surface. The GC case has larger vertical velocity variance at high wavenumbers, and this may be an effect of the rolls contributing to the turbulence spectrum (the rolls have relatively large characteristic length scale). However, the resulting difference in variance between the two cases is still rather small. At the top of the CBL, there is very little difference between the spectra at moderate to high wavenumbers (in the inertial subrange). However, the GC case has notably higher variance at length scales on the order of the boundary layer depth, in the small wavenumber range. The increase in energy at low wavenumbers in the spectra is consistent with the extra turbulence kinetic energy production by shear.



(a) (b)
Figure 5. Structure of the u , v , and w fields for the (a) NS and (b) GS cases, both with 20500s into the simulation.



(a) (b)
Figure 6. Turbulence spectra at the top of the boundary layer for the NS and GC cases (a) near the surface and (b) at the top of the CBL.

4 CONCLUSIONS

The mean wind profiles and turbulence structure are strongly influenced by wind shear within the CBL. In particular, the CBL growth rate, as well as shear in the geostrophic wind, has a sig-

nificant influence on the evolution of the mean wind field. The CBL evolution with constant geostrophic forcing is generally characterized by winds within the growing boundary layer slowing to speeds less than geostrophic. If the geostrophic wind is zero at the surface and grows rapidly upwards, the CBL winds at first become subgeostrophic and then increase, as, in the process of CBL growth, more momentum is mixed down into the core of the CBL. Organized CBL flow structures look significantly different in the presence of shear, with the most significant differences existing between the no-shear (NS) and the constant geostrophic forcing (GC) cases, where the differences are greatest at the surface. The simulations performed are consistent with the results of earlier modeling studies, indicating hexagonal cells for the NS case and horizontal rolls for the GC case as dominant turbulence structures in the lower portion of the CBL. Despite the great difference in structure, the spectra do not differ significantly, except, for somewhat less amplitude at moderate and high wavenumbers and slightly greater amplitude at low wavenumbers in the GC case. At the CBL top, the increase in energy at low wavenumbers is consistent with the added turbulence kinetic energy production by shear.

5 ACKNOWLEDGEMENTS

The authors would like to thank the National Science Foundation (grant ATM-0124068) for funding the research that led to this publication.

6 REFERENCES

- 1 S .P. S. Arya and J C. Wyngaard, Effect of baroclinicity on wind profiles and the geostrophic drag law for the convective planetary boundary layer, *Journal of the Atmospheric Sciences*, 32 (1975) 767-778.
- 2 A. R. Brown, Large-eddy simulation and parametrization of the baroclinic boundary-layer, *Quarterly Journal of the Royal Meteorological Society*, 122 (1996) 1779-1798.
- 3 J R. Garratt and J. C. Wyngaard, Winds in the atmospheric convective boundary layer – prediction and observation, *Journal of the Atmospheric Sciences*, 39 (1982) 1307-1316.
- 4 L. R. Hoxit, Planetary boundary layer winds in baroclinic conditions, *Journal of the Atmospheric Sciences*, 31 (1974) 1003-1020.
- 5 M. A. Lemone, M. Zhou, C.-H. Moeng, D. H. Lenschow, L. J. Miller, and R. L. Grossman, An observational study of wind profiles in the baroclinic convective mixed layer, *Boundary Layer Meteorology*, 90 (1999) 47-82.
- 6 S. K. Pedersen and G. D. Stubbley, A scaling parameter for turbulence in baroclinic boundary layers, *Boundary Layer Meteorology*, 68 (1994) 319-325.
- 7 B. Stevens and J. Duan, Entrainment, Rayleigh friction, and boundary layer winds over the tropical Pacific, *Journal of Climate*, 15 (2002) 30-44.
- 8 C.-H. Moeng and P. P. Sullivan, A comparison of shear- and buoyancy-driven planetary boundary layer flows, *Journal of the Atmospheric Sciences*, 51 (1994) 999-1022.
- 9 S. Khanna and J. G. Brasseur, Three-dimensional buoyancy and shear-induced local structure of the atmospheric boundary layer, *Journal of the Atmospheric Sciences*, 55 (1998) 710-743.
- 10 H. Schmidt and U. Schumann, Coherent structure of the convective boundary layer derived from large eddy simulations, *Journal of Fluid Mechanics*, 200 (1989) 511-562.
- 11 Z. Sorbjan, Effects cause by varying the strength of the capping inversion based on a large eddy simulation model of the shear-free convective boundary layer, *Journal of the Atmospheric Sciences*, 53 (1996) 2015-2024.
- 12 J. W. Deardorff, Stratocumulus-capped mixed layers derived from a three-dimensional model, *Boundary Layer Meteorology*, 18 (1980) 495-527.
- 13 J. C. Wyngaard and R. A. Brost, Top-down and bottom-up diffusion of a scalar in the convective boundary layer, *Journal of the Atmospheric Sciences*, 41 (1984) 102-112.
- 14 F. T. M. Nieuwstadt and R. A. Brost, The decay of convective turbulence, *Journal of the Atmospheric Sciences*, 43 (1986) 532-546.